Vortex dissipation in $Y_{1-x}Pr_xBa_2Cu_3O_{7-\delta}$ superconductors above and below the zero-field critical temperature

T. Katuwal, V. Sandu,* and C. C. Almasan
Department of Physics, Kent State University, Kent, Ohio 44242, USA

B. J. Taylor and M. B. Maple
Department of Physics, University of California at San Diego, La Jolla, California 92093, USA
(Received 9 May 2005; revised manuscript received 4 August 2005; published 2 November 2005)

We investigated in-plane angular magnetoresistivity $\Delta\rho_{ab}/\rho_{ab}(0°)$ below and above the zero-field critical temperature T_{c0} of $Y_{1-x}Pr_xBa_2Cu_3O_{7-\delta}$ single crystals with $0.0 \leqslant x \leqslant 0.53$. The angular dependence of in-plane magnetoresistivity shows three temperature regimes: (a) a low T regime which extends from below to above the critical temperature T_{c0}, up to an x-dependent temperature (e.g., up to $1.15 \times T_{c0}$ for $x=0.46$), displaying a two-dimensional (2D) scaling (consistent with pancakelike excitation), (b) an intermediate T regime, corresponding to vortex line excitations, which extends up to $T_\varphi > T_{c0}$, and (c) a high T regime in which the quasiparticles dominate the dissipation. The constructed electronic phase diagram shows that $T_\varphi(x)$ departs from $T_{c0}(x)$ for $x \geqslant 0.20$ and reaches a maximum at $x=0.46$.

DOI: 10.1103/PhysRevB.72.174501 PACS number(s): 74.25.Fy, 71.30.+h, 74.72.Bk, 75.47.Gk

I. INTRODUCTION

The most striking relationship between superconductivity and normal state of cuprates is observed in systems with reduced charge carrier density, i.e., in underdoped materials. In these materials, the main feature of the normal state is the reduced $\vec{k}$ dependent quasiparticle density of states (DOS) known as pseudogap, which was experimentally observed by nuclear magnetic resonance (NMR), angle-resolved photoemission spectroscopy (ARPES), neutron scattering, Raman spectroscopy, scanning tunneling spectroscopy (STS), and transport measurements (see the review of Timusk and Statt[1] and references therein), making questionable even the name of "normal state."

The superconducting state, on the other hand, shows strong fluctuations caused not only by the effective low dimensional electron spectrum and relative high critical temperature, but also by the diminished concentration of superconducting charge carriers n_s. The corresponding reduced stiffness $\hbar n_s/4m^*$ emphasizes the role of phase fluctuations of the superconducting order parameter relative to the amplitude. Additionally, ARPES (Ref. 2) and STS (Ref. 3) experiments have shown that the gap evolves smoothly through the superconducting critical temperature T_{c0}. As a consequence, there is a temperature range $T_{c0} < T < T_\varphi$, where the order parameter has constant amplitude, $\Psi(x)=\Psi_0 e^{i\varphi}$, but zero average,[4] $\langle\Psi\rangle=0$, and where the correlator $\langle\Psi(0,0)\Psi(\vec{r},\tau)\rangle$ remains nonzero within a certain coherence length[5,6] and time.[7] Cooper pairs still survive[8] up to a higher temperature $T^* > T_\varphi$, but without any phase coherence.

Because the superconducting fluctuation regime overlaps with the pseudogap regime over a large temperature range above T_{c0}, the latter was intimately connected to the phase fluctuation of the order parameter and depicted as a normal state where the quasiparticle spectrum is controlled by the superconducting phase fluctuations.[9–15] In this conjecture, T_{c0} is the phase coherence temperature and the "normal" pseudogaped state is conceived as a mixture of free (anti) vortices and quasiparticles where the former renormalize the quasiparticle DOS producing a rapid spectral broadening.[10] It is noteworthy that this process is possible due to the d wave symmetry of the superconducting order parameter, because the dominant interaction comes from the nodal quasiparticles. Experimental evidence supporting this model is considerable and involves the finite high frequency and microwave imaginary conductivity above T_{c0} found in underdoped cuprates,[16,17] the anomalous fluctuation diamagnetism,[18] the large Nernst effect observed well above T_{c0},[19–22] the anomalous hysteresis in the T dependence of the magnetization reported in the same temperature range,[23] and the angular magnetoresistivity measurements.[24]

All the experiments mentioned above were interpreted as evidence of vorticity above the critical temperature of the superconducting cuprates. However, the literature lacks information regarding the dissipation mechanisms of the vortex and quasiparticle systems in the pseudogap regime, above the zero-field critical temperature. In this temperature range both contributions to dissipation have to be treated on equal footing regarding the charge transport process. Indeed, it has been shown that even in the optimally doped cuprates, close to T_{c0}, the flux-flow resistivity increases fast to the normal state resistivity despite the existence of a still large amount of condensate.[25] Angular magnetoresistivity AMR experiments have the advantage that they permit the simultaneous determination of the main features of *both* vortex excitations and quasiparticles as they manifest themself in the charge transport processes. It seems that the price paid for this advantage is a lower sensitivity in the AMR experiments as compared to other experiments dedicated to the detection of only one system, like Nernst-effect measurements which are sensible only to the motion of vortices.

This paper is a detailed study of the nature of vortex dissipation over a wide range of temperatures and magnetic fields in underdoped single crystals of $Y_{1-x}Pr_xBa_2Cu_3O_{7-\delta}$

for a large selection of Pr concentrations ($0.0 \leqslant x \leqslant 0.53$). We show that vortexlike excitations follow a two-dimensional (2D) scaling law from $T < T_{c0}$ up to a certain temperature higher than T_{c0} (for example, up to $1.15 \times T_{c0}$ for $x=0.46$), cross to a three-dimensional (3D) behavior at higher temperatures, and vanish above a temperature $T_{\varphi} > T_{c0}$. The difference $T_{\varphi} - T_{c0}$ is doping x dependent, displaying a maximum for $Y_{0.54}Pr_{0.46}Ba_2Cu_3O_{7-\delta}$. The evolution with temperature, magnetic field, and doping of quasiparticle ordinary magnetoresistivity and flux-flow resistivity is also studied.

II. EXPERIMENTAL DETAILS

We performed electrical transport measurements using a Quantum Design physical property measurement system (PPMS) on $Y_{1-x}Pr_xBa_2Cu_3O_{7-\delta}$ single crystals grown as described in Ref. 26. Typical sizes of the single crystals under investigation are $1.0 \times 0.5 \times 0.02$ mm^3, with the c axis oriented along the smallest dimension. Four gold leads with a diameter of 0.025 mm were attached, using silver paste, on each face of the crystal. In-plane ρ_{ab} and out-of-plane ρ_c resistivities were measured simultaneously using this multiterminal configuration. Specifically, a current $I \leqslant 0.1$ mA was applied on one face of the single crystal and the voltages on both faces were measured with a low frequency (16 Hz) ac bridge. The components of the resistivity tensor were extracted from these voltages using the algorithm described in Ref. 27. For the measurements in magnetic field, we chose a system with the z axis along the crystallographic c axis and x axis along the driving current I, which is also one of the in-plane crystallographic axis. The dependence of the resistivity on the polar angle $\rho(\theta)$ was determined for zero azimuthal angle $\phi=0$, at constant temperature T and applied magnetic field H up to 14 T by rotating the single crystal from $H \| (\theta=0°)$ to $H \| (ab) \| I (\theta=90°)$. The Hall contribution was subtracted using symmetry considerations.

III. RESULTS AND DISCUSSIONS

Figure 1 shows the temperature dependence of ρ_{ab} of $Y_{1-x}Pr_xBa_2Cu_3O_{7-\delta}$ single crystals measured in zero-magnetic field. The zero-field critical temperature T_{c0}, defined here as the temperature corresponding to the inflection point in the transition region, decreases from 92 K ($x=0$) to 13 K ($x=0.53$) while the resistivity increases. For $x=0$, ρ_{ab} exhibits a parabolic T dependence, corresponding to a slight overdoping. The dependence becomes linear in T for $x=0.13$ while for higher Pr concentrations shows the typical pseudogap bump. Namely, $\rho_{ab}(T)$ has a slower than linear T dependence at high temperatures (even logarithmic behavior at high x values), a faster decrease below the bump, and slows down or starts to increase before the superconducting transition temperature.

The increase of the resistivity and the depression of T_{c0} with increasing x is the result of the reduction in the number of free holes, which get localized in the Fahrenbacher-Rice (FR) band resulting from the p-f hybridization.[28] Computations based on the existence of p-f hybridization have shown

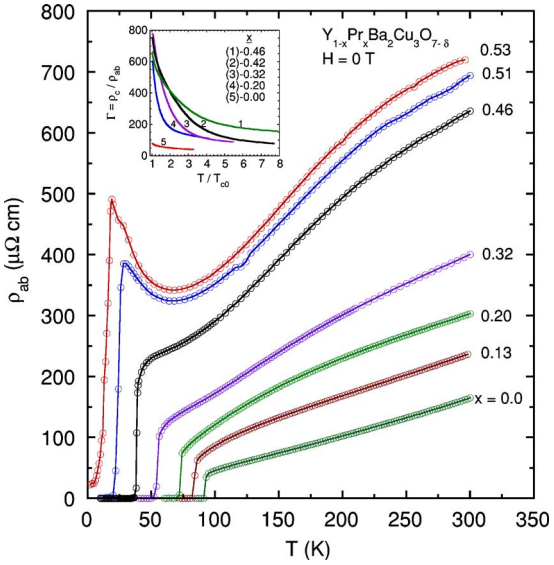

FIG. 1. (Color online) The temperature T dependence of in-plane resistivity ρ_{ab} of $Y_{1-x}Pr_xBa_2Cu_3O_{7-\delta}$ single crystals for different Pr concentrations x measured in a zero magnetic field. Inset: Temperature T dependence of resistive anisotropy $\Gamma = \rho_c / \rho_{ab}$ for different concentrations x. The solid lines are guides to the eye.

that the hole reduction with increasing Pr content is mainly due to hole transfer from the $pd\sigma$ band of CuO_2 planes to the FR band, with a very small effect on the number of holes in the CuO chains.[29] However, the FR band forms only above a certain threshold of Pr content x, most likely for $x > 0.15$ (hole density, i.e., number of holes per Cu site in the CuO_2 planes, $h < 0.26$ holes/Cu). For lower x values, the small decrease of the critical temperature of $Y_{1-x}Pr_xBa_2Cu_3O_{7-\delta}$ with decreasing x is rather a result of the disorder associated with the random substitution of Pr for Y. In this case, i.e., for low Pr content, the doping is controlled only by the amount of oxygen in the chains. This is the case of the $x=0.13$ sample; the linear ρ_{ab} vs T dependence shows that hole doping is optimal in this single crystal.

The out-of plane resistivity of the $x=0$ single crystals shows metallic behavior for all $T > T_{c0}$ while $\rho_c(T)$ of single crystals with a higher Pr content display a crossover from metallic to nonmetallic behavior (data not shown). Details regarding the behavior of $\rho_{ab}(T,x)$ and $\rho_c(T,x)$ as a function of doping x, of similar single crystals, are given in Ref. 30.

The inset to Fig. 1 is a plot of the anisotropy $\Gamma = \rho_c / \rho_{ab}$, as extracted from the normal state resistivities vs the reduced temperature T/T_{c0}, for different Pr concentrations. The anisotropy increases with decreasing T as a result of the reduction of the DOS starting at $\vec{k}=(\pi,0)$ points of the Brillouin zone, which affects more ρ_c than ρ_{ab}. For a given doping, we take the anisotropy in the superconducting state, $\gamma = m_c/m_{ab}$, as $\gamma = \sqrt{\Gamma}(T \approx T_{c0})$, since this value of $\sqrt{\Gamma}$ is close to the value of the anisotropy in the superconducting state γ as obtained from the T dependence of the melting field[31] and from Josephson flux-flow experiments.[32]

Recent angular dependent in-plane resistivity measurements on $Y_{1-x}Pr_xBa_2Cu_3O_{7-\delta}$ single crystals with $x \geqslant 0.2$ have shown that a strong deviation from a $\sin^2\theta$ dependence

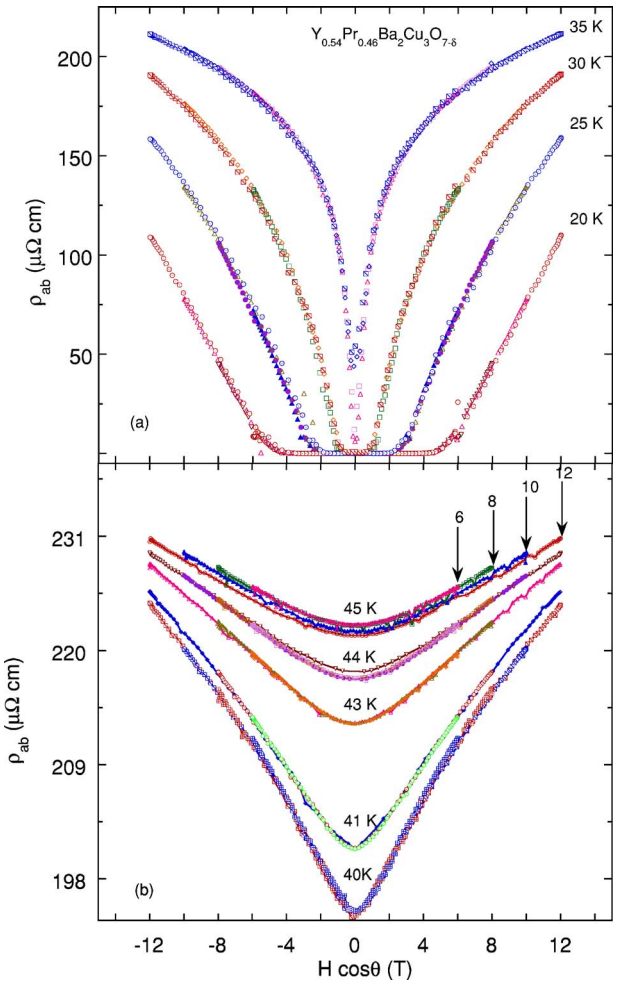

FIG. 2. (Color online) The scaling of the resistivity ρ_{ab} vs $H\cos\theta$ curves of $Y_{0.54}Pr_{0.46}Ba_2Cu_3O_{7-\delta}$ single crystal measured at 6, 8, 10, and 12 T (a) 20, 25, 30, and 35 K, and (b) 40, 41, 43, 44, and 45 K.

(a result expected from quasiparticle dissipation), which increases with decreasing T, appears below a certain temperature $T_\varphi > T_{c0}$ and continues also below T_{c0}.[24] We have shown that this deviation is consistent with the presence of flux vortices over this whole T range, hence, even above T_{c0}.[24] A question that still remains is what is the nature of the flux vortices over this T range and how does the dissipation due to flux flow and quasiparticles change with temperature and magnetic field.

It has been shown that vortex dissipation in the superconducting state of highly anisotropic cuprates follows a two-dimensional behavior (the magnetic field applied along the c axis penetrates in the form of quasi-2D Josephson coupled pancakes) over a wide temperature range in which the c axis coherence length ξ_c is smaller than the interlayer spacing s.[33] Therefore, the 2D vortex dissipation depends only on, hence scales with, the component of the magnetic field perpendicular to the ab planes, i.e., $H\cos\theta$. This 2D scaling law has already been observed experimentally below T_{c0} in optimally doped cuprates with large anisotropy.[34–36] Figures 2(a) and 2(b) are plots of in-plane resistivity of the $x=0.46$ single crystal ($T_{c0}=38$ K) vs $H\cos\theta$ measured at temperatures both below [Fig. 2(a)] and above [Fig. 2(b)] T_{c0} and in applied magnetic fields of 6, 8, 10, and 12 T. The data follow very well the above scaling law over an extended temperature range, below T_{c0} (for 20 K$\leqslant T\leqslant$38 K) but also several degrees above T_{c0} (up to 44 K for this Pr doping), and over the whole range of angles except for the strictly parallel configuration $H\|I\|ab$, i.e., $\theta=90^0$. This result indicates that, even above T_{c0}, the flow of 2D vortices dominates the dissipation. For temperatures $45\leqslant T<60$ K, the $H\cos\theta$ scaling fails [for example, see the data at 45 K in Fig. 2(b)]. The failure of the scaling at these higher temperatures could be the result of a 2D→3D crossover, where ρ_{ab} follows different field and angle dependences and the flux line picture appears to be more appropriate.

Notice that the resistivity data of Figs. 2(a) and 2(b) which scale with $H\cos\theta$ are proportional to $H\cos\theta$, as expected for bare 2D vortex dissipation,[33] at 20 K, while at $T\geqslant 25$ K they show a negative curvature which is maintained even above T_{c0}, i.e., in the most general form

$$\rho_{ab} \propto \mathcal{Z}(H|\cos\theta|). \tag{1}$$

We show in the Appendix that the negative curvature of $\mathcal{Z}(H|\cos\theta|)$ and its evolution with temperature are the result of the interplay between the temperature dependences of the quasiparticle and flux-flow channels in the total resistivity. In addition, note that for $H|\cos\theta|<1$ and $T<T_{c0}$, the function $\mathcal{Z}(H|\cos\theta|)$ evolves fast towards a cusplike minimum ($d\rho_{ab}/d\theta|_{\theta=90^\circ}\neq 0$) at $\theta=90^\circ$, but does not follow the linear decrease ($\mathcal{Z}\propto|90^\circ-\theta|$) when $\theta\to 90^\circ$ (as expected for bare flux flow), which further indicates the presence of another contribution to dissipation. With increasing temperature, the cusp crosses smoothly into a more and more rounded dip, $d\rho_{ab}/d\theta|_{\theta=90^\circ}=0$, probably due to the thermal wandering of the Josephson flux lines. All these experimental facts of Fig. 2 suggest that the 2D behavior is not lost at T_{c0}, i.e., not only that the c axis coherence length does not diverge at T_{c0}, but in fact it remains smaller than the interlayer spacing up to 44 K.

The nonvanishing resistivity at $\theta=90^0$, i.e., when $H\|I$, which is present even below T_{c0} [see Fig. 2(a)], is most likely due to the movement of the pancake vortices associated with the kinks generated by the thermally excited excursions of the Josephson lines in the adjacent interlayer spacing. This wandering is the result of the exponential weakening of the intrinsic pinning potential[37] U_p when $\xi_c\to s$, which proliferates kinks, i.e., 2D vortices, with a kink density per line $\propto L_k^{-1}\propto\gamma(k_BT/s\epsilon_0)$.[38] Here L_k is the distance between two successive kinks and $\epsilon_0=\Phi_0^2/(4\pi\mu_0\lambda^2)$.

Based on the above discussion, we assume that the flux-flow resistivity has two different expressions dictated by the dimensionality of the vortex matter. Namely, at temperatures corresponding to the 2D vortex regime, where $\xi_c<s$, the vortex dissipation follows the expression:

$$\rho_{ab,FF}=\rho_0\frac{H|\cos\theta|}{\eta H^*}+\beta\rho_{ab,qp}. \tag{2}$$

Here $H^*=H^*(0)(1-T/T_\varphi)$ is the scaling field, since it is more appropriate to use H^* instead of the mean field upper critical

field H_{c2} to depict the fluctuation regime.[21,39] At high temperatures, where $\xi_c > s$, the flux dissipation becomes 3D and it follows the expression:[24]

$$\rho_{ab,FF} = \rho_0 H \sum_i \frac{p_i \vartheta(H_i^* - H)}{\eta_i H_i^*(T, \theta = 0)} |\cos\theta| \sqrt{\cos^2\theta + \frac{\sin^2\theta}{\Gamma}} + \beta \rho_{ab,qp}. \quad (3)$$

Here, the resistivity is a result of flux flow dissipation in superconducting regions (islands) of size of the order of the phase correlation length ξ_φ [where $\langle \Psi(0)\Psi(\vec{r},\tau)\rangle$ is finite] connected by nonsuperconducting regions. The phase correlation length is maximum at T_{c0} and vanishes at T_φ. We note that the term "island" is a space and time generalization, and it means a certain size r and a certain life time τ. For the sake of generality, we assume that each superconducting "island" has a weight p_i and is characterized by its own scaling field H_i^* and viscosity η_i; $\vartheta(x)$ is the Heaviside function,

$$\vartheta(x) = \begin{cases} 0 & \text{for } x < 1, \\ 1 & \text{for } x > 1. \end{cases}$$

The second term, $\beta\rho_{ab,qp}$, of Eqs. (2) and (3) accounts either for the serial resistances connecting nonpercolating superconducting "islands" along a current path (including also the normal superconductor interface resistivity) or for the dissipation arising from the thermally excited kinks of Josephson vortices. The coefficients p_i, η_i, and β are temperature and field dependent.

We note that, in the type of inhomogeneity introduced above, the superconducting and nonsuperconducting regions fluctuate in space and time as a result of the holes redistribution within the sample in order to minimize their energy in the potential induced by the doping. Such an intrinsic inhomogeneity is not putative and the existence of Meissner "islands" with very long life time, up to $4 \times T_{c0}$, was visualized in superconducting quantum interference device (SQUID) microscopy experiments on underdoped $La_{2-x}Sr_xCuO_4$.[40] It is also supported by the the space variation of the gap parameter as obtained from scanning tunneling microscope (STM) experiments.[41,42]

Next, we obtain an explicit functional dependence of magnetoresistivity which is consistent with the 2D and 3D vortex matter and study the evolution of different characteristics of dissipation with magnetic field, temperature, and doping. We have shown above that the convexity of the resistivity [see Eq. (1)] and its evolution with temperature are the result of the presence of both quasiparticles and flux-flow channels in the total resistivity. Therefore, we assume that the total conductivity measured experimentally is given by these two channels which are connected in parallel; i.e., $\sigma_{ab}(T,H,\theta) = \sigma_{ab,qp}(T,H,\theta) + \rho_{ab,FF}^{-1}$. Here, the flux-flow term is given by Eq. (2) or Eq. (3) when the vortex matter is 2D or 3D, respectively. The H and T dependence of the quasiparticle conductivity σ_{qp} in the pseudogap state is rather complex because the Fermi surface is a fourfold symmetric cylinder slightly warped along the k_z axis. However, within Boltzmann approximation and if one neglects the slow variation of the k_z component of the Fermi momentum k_F, the Jones-Zener expansion gives a $\cos^2\theta$ dependence for the field contribution to the quasiparticle conductivity (see for example Hussey[43]); i.e.,

$$\sigma_{ab,qp}(T,H,\theta) = \sigma_{ab,qp}^0(T) - \sigma_{ab}^{(2)}(T) H^2 \cos^2\theta, \quad (4)$$

where σ^0 and $\sigma^{(2)}$ are the first two terms of the Jones-Zener series of the conductivity in powers of H. Moreover, since magnetoresistivities are given directly by magnetoconductivities with inverted sign,[44] it follows that the total measured angular magnetoresistivity is given by

$$\frac{\Delta\rho_{ab}^{anis}}{\rho_{ab}} \approx -\frac{\Delta\sigma_{ab,qp}}{\sigma_{ab}(0^\circ)} - \frac{\Delta\sigma_{ab,FF}}{\sigma_{ab}(0^\circ)} = -M_{qp}\sin^2\theta - \frac{\Delta\sigma_{ab,FF}}{\sigma_{ab}(0^\circ)}, \quad (5)$$

where $M_{qp} \equiv \sigma^{(2)} H^2/\sigma_0$ is the ordinary magnetoresistivity, i.e., $\sigma(H) - \sigma(0)$, of the quasiparticles [see Eq. (4)]. In this equation,

$$\frac{\Delta\sigma_{ab,FF}}{\sigma_{ab}(0^\circ)} = \frac{M_{FF}}{|\cos\theta| + \beta M_{FF}(1 + M_{qp}\cos^2\theta)} - \frac{M_{FF}}{1 + \beta M_{FF}(1 + M_{qp})} \quad (6)$$

for the 2D regime, when $\rho_{ab,FF}$ is given by Eq. (2) and $M_{FF} = \eta H^*/H$, or

$$\frac{\Delta\sigma_{ab,FF}}{\sigma_{ab}(0^\circ)} = \frac{M_{FF}}{|\cos\theta|\sqrt{\cos^2\theta + \frac{\sin^2\theta}{\Gamma}} + \beta M_{FF}(1 + M_{qp}\cos^2\theta)} - \frac{M_{FF}}{1 + \beta M_{FF}(1 + M_{qp})} \quad (7)$$

for the 3D regime, when $\rho_{ab,FF}$ is given by Eq. (3) and $M_{FF}^{-1} \equiv H\Sigma_i[p_i\vartheta(H_i^* - H)]/[\eta_i H_i^*(T, \theta = 0)]$. Both M_{qp} and M_{FF} are temperature- and field-dependent coefficients for the quasiparticle and flux-flow contributions, respectively.

Equation (5) with $\Delta\sigma_{ab,FF}/\sigma_{ab}$ given by Eq. (6) gives an excellent fit to the measured in-plane angular magnetoresistivity (AMR) for all temperatures at which the resistivity data show the $H\cos\theta$ scaling [see Fig. 3(a) for the $x = 0.46$ single crystal ($T_{c0} = 38$ K)]. In this temperature range, which extends above T_{c0}, the 2D vortices dominate the dissipation. As also shown previously,[24] Eq. (5) with $\Delta\sigma_{ab,FF}/\sigma_{ab}$ given by Eq. (7) gives an excellent fit to the measured in-plane AMR for higher temperatures, where the $H\cos\theta$ scaling fails, up to a temperature T_φ [see Fig. 3(b) for the $x = 0.46$ single crystal ($T_{c0} = 38$ K, $T_\varphi = 58.5$ K)]. The flux-flow contribution (M_{FF}) to AMR decreases as the temperature increases and, finally, at T_φ becomes negligible compared with the quasiparticle contribution. We used the χ^2 criterion to determine T_φ by comparing the fits with Eq. (5) and with $M_{qp}\sin^2\theta$ alone. The latter provides a better fit of the data for $T > T_\varphi$. All these results are true for single crystals with $x \geq 0.20$.

For smaller Pr concentrations, i.e., for the $x = 0$ and 0.13 single crystals, the in-plane AMR displays only a $\sin^2\theta$ dependence over the whole measured T range. The reason

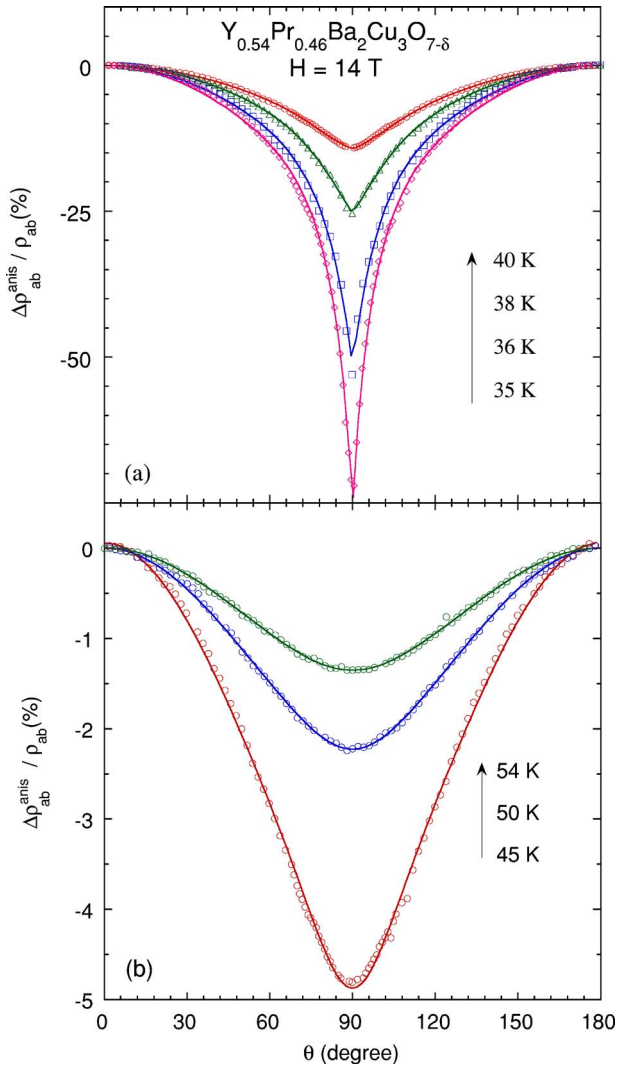

FIG. 3. (Color online) The in-plane angular magnetoresistivity $\Delta\rho_{ab}^{anis}/\rho_{ab}(0°) \approx [\rho_{ab}(\theta) - \rho_{ab}(0°)]/\rho_{ab}(0°)$ vs angle θ between the magnetic field H and the c axis, measured at 14 T and at (a) 35, 36, 38, and 40 K, and (b) 45, 50, and 54 K for the $x=0.46$ single crystal. The solid lines in (a) and (b) are fits of the data with Eq. (5) in which the flux-flow conductivity is given by Eqs. (6) and (7), respectively.

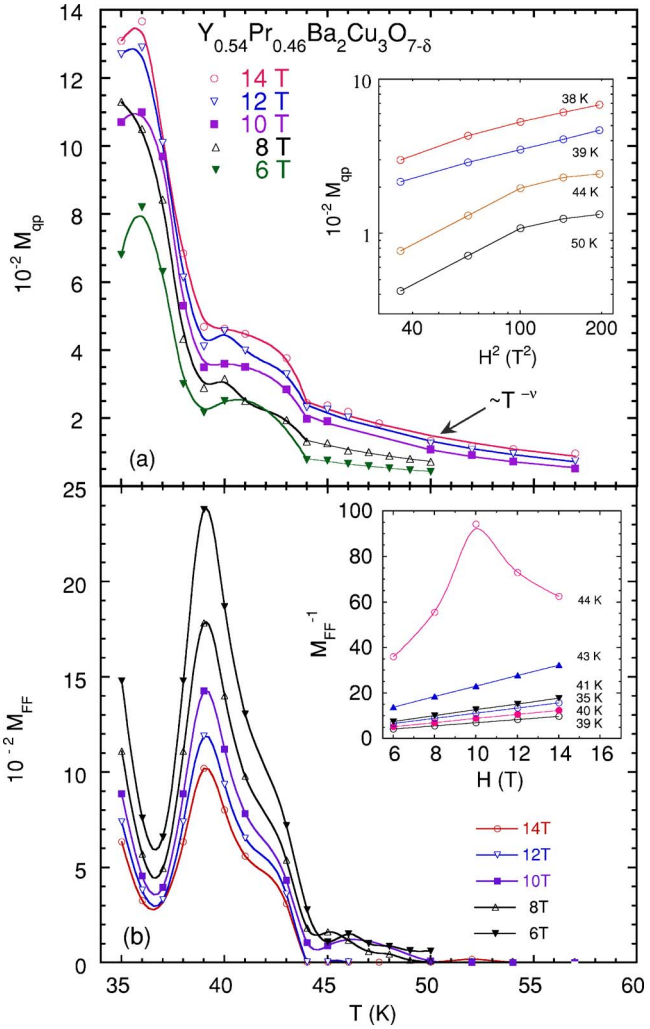

FIG. 4. (Color online) The temperature T (main panels) and magnetic field H (insets) dependences of the (a) M_{qp} and (b) M_{FF} coefficients, for the $x=0.46$ sample. The solid lines are guides to the eye.

could be the following. In this regime of high hole concentration, the fluctuations are Gaussian and their extension is limited to a temperature range around T_{c0}. The high stiffness and reduced anisotropy make the excitation of phase fluctuations less probable due to the high energetic cost. Therefore, both phase and amplitude fluctuations of the order parameter have the same temperature scale and T_{c0} is both the pairing and the coherence temperature. In this case, the presence of phase fluctuations is practically negligible, the normal state is characterized by a well-defined Fermi surface down to T_{c0}, and conductibility is practically limited to the quasiparticle term, which follows a $\cos^2\theta$ angular dependence, hence, the AMR follows a $\sin^2\theta$ dependence.

The evolution with temperature and magnetic field of the quasiparticles ordinary magnetoresistivity and of the flux-flow angular magnetoresistivity is given by the temperature and field dependence of M_{qp} and M_{FF}, respectively. The temperature dependence of the fitting coefficients M_{qp} and M_{FF} is shown in Figs. 4(a) and 4(b), respectively, while the inset to each figure shows the field dependence of each coefficient. M_{qp} [Fig. 4(a)], namely the quasiparticle ordinary magnetoresistivity, decreases monotonically with increasing temperature for all magnetic fields between 6 and 14 T. This decrease is fast for $T<T_{c0}$ while, for $T>44$ K, it follows roughly a power law, i.e., $M_{qp} \propto T^{-\nu}$. The exponent ν decreases weakly with increasing field, i.e., $\nu(H=4\text{ T}) \approx 5.3$ and $\nu(H=14\text{ T}) \approx 4$. This T dependence of the quasiparticle ordinary magnetoresistivity is consistent with theoretical considerations. Indeed, simple considerations based on Boltzmann's equation give $M_{qp} \propto \tau^2$ where τ is the relaxation time for quasiparticles. Therefore, the fast decrease of M_{qp}, hence ordinary magnetoresistivity, with increasing T for $T<T_{c0}$, is a result of the increase of the phase space for scattering with increasing temperature.[45] On the other hand, in the approximation of a Fermi liquid with anisotropic relaxation time, it has been proposed that $\nu=4$ for $T>T_{c0}$,[46]

while a more elaborate Fermi liquid model, which takes also into account renormalization due to the antiferromagnetic fluctuations,[47] shows that the quasiparticle ordinary magnetoresistivity changes even faster than T^{-4}.

In the high temperature regime, M_{qp} is linear in H^2 up to 10 T and saturates at higher fields [see the inset to Fig. 4(a)]. The $M_{qp} \propto H^2$ dependence is consistent with its definition, i.e., $M_{qp} \equiv \sigma^{(2)} H^2 / \sigma_0$, and hence supports the validity of the expression chosen for the quasiparticle conductivity given by Eq. (4). The saturation of $M_{qp}(H)$ is in agreement with the $\rho_{ab}(H)$ data (not shown). According to Fermiologic considerations,[48] a saturation of quasiparticle ordinary magnetoresistivity is expected for closed orbits in $\vec{k}$ space, which in the case of cuprates occurs for the whole explored angular range except $\theta = 90^{\circ}$ because of the almost cylindrical geometry of the Fermi surface.

The temperature dependence of the phase fluctuation channel term, M_{FF}, which is inverse proportional with the flux-flow resistivity, is shown in Fig. 4(b). The peak in $M_{FF}(T)$ around T_{c0} is the result of the temperature dependence of the viscosity η [see the expression of M_{FF} for Eq. (6)]. The swelling of the vortices with increasing T reduces the diffusion relaxation rate of the order parameter and of the associated quasiparticle excitations.[49] Hence, the viscosity increases as $\eta \propto (1 - T/T_{c0})^{-1/2}$. At a certain temperature, the diffusion relaxation rate becomes equal to the inelastic relaxation rate of the quasiparticle excitations, hence the viscosity reaches a maximum. For even higher temperatures, the latter process dominates the relaxation and the viscosity starts to decrease as $\eta \propto (1 - T/T_{c0})^{1/2} T_{c0} \tau_{ph}$, where τ_{ph} is the phonon-excitation scattering time. Three other reasons for the decrease of $M_{FF}(T)$ for $T > T_{c0}$ are: the fast decrease of the scale over which vortex pairs unbind,[50,51] the rapid reduction of the phase correlation length ξ_{φ}, which decreases the number of "islands" able to support vorticity, and the faster increase above T_{c0} of the radius of the outer limit of the vortex core compared to ξ_{ab}, as revealed by Nernst effect experiments.[21]

Interestingly, a shoulder is clearly present in the $M_{FF}(T)$ around 43–44 K, the temperature at which the 2D to 3D crossover in the vortex matter is observed (see Fig. 2). Therefore, the reason for this shoulder, i.e., decrease in vortex dissipation, could be the increase in vortex line rigidity relative to the pancake vortices, hence decrease in vortex mobility, as a result of the increase in dimensionality.

The field dependence of M_{FF}^{-1} is linear at low temperatures ($T \leqslant 44$ K) [see the inset to Fig. 4(b)], as predicted by its definition in Eqs. (6) and (7). At higher temperatures, however, M_{FF}^{-1} is nonmonotonic, decreasing above a certain field. These results could be explained as follows. At low temperatures, as H increases, the number of vortices increases, hence vortex dissipation and M_{FF}^{-1} increase linearly with H. At higher temperatures, the number of regions able to support vorticity is not constant but decreases with increasing H. As a result, the number of vortices introduced by the field in the more robust regions is smaller than the number of vortices lost as a result of the vanishing of the weaker regions. Hence, the overall effect is a decrease of M_{FF}^{-1}, hence vortex dissipation with increasing H.

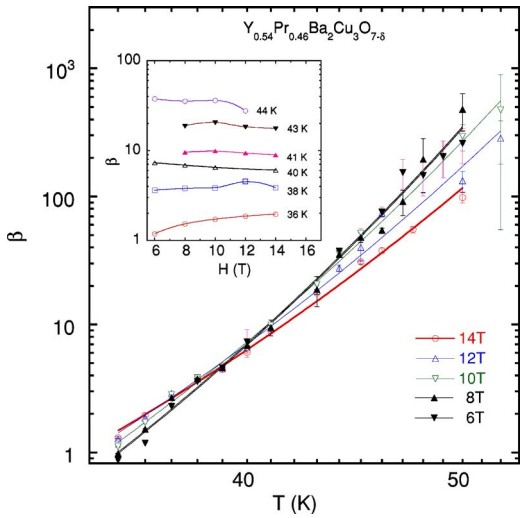

FIG. 5. (Color online) The temperature T (main panel) and magnetic field H (inset) dependences of the coefficient β for the $x = 0.46$ sample. The solid lines are guides to the eye.

The temperature and field dependence of β is shown in Fig. 5 and its inset, respectively. The parameter β shows an exponential increase with T over the whole temperature range ($35 \leqslant T \leqslant 57$ K) and a weak dependence on H. The origin of this term could be both in the fluctuation of the Josephson lines, which produces finite resistance at $\theta = 90°$, as well as in the nonsuperconducting islands. The exponential increase of β with increasing T indicates a decrease with T of the phase correlation length ξ_{φ}, which determines the size of the superconducting islands. The slight reduction in $\beta(H)$ at high T could be explained by the field reduction of the normal superconducting interface resistance due to the charge imbalance.

Next, we discuss the effect of Pr doping x on magnetoresistivity. We obtained the relationship between the praseodymium content x and the hole density h, i.e., the number of holes per Cu site in the CuO_2 planes, from μSR[52] and neutron scattering[53] data. Figure 6 is a plot of the zero-field critical temperature T_{c0}, the 2D-3D crossover temperature T_{cr}, and the temperature T_{φ} at which the phase correlations vanish, as a function of the hole density h. We also indicate on the figure the value of the doping x for each single crystal. This plot provides an overview of how high in temperature, above T_{c0}, the 2D-3D crossover takes place and the vortex-like excitations extend for various hole densities. Notice that $T_{cr}(h)$ and $T_{\varphi}(h)$ tracks $T_{c0}(h)$. Note that $T_{cr} \approx 1.15 \times T_{c0}$ for the strongly underdoped samples, which have higher anisotropy, and it approaches T_c as the anisotropy decreases. The values of T_{φ} are, over an extended concentration range, i.e., $0.32 \leqslant x \leqslant 0.47$, in good agreement with an estimated value of $T_{\varphi} \approx 1.5 \times T_{c0}$ obtained based on the anisotropic 3D-XY model.[5] At high hole densities (low Pr content) both $T_{\varphi}(h)$ and $T_{c0}(h)$ curves merge. At very low hole density both curves display an abrupt decrease, but the two temperatures do not merge. As a result, the temperature range of phase fluctuations $\Delta T_{\varphi} \equiv T_{\varphi} - T_{c0}$ displays a maximum around $x = 0.46$ (see the inset to Fig. 6).

We note some differences between the present data and the Nernst effect[20] and magnetization vs T data,[23] reported

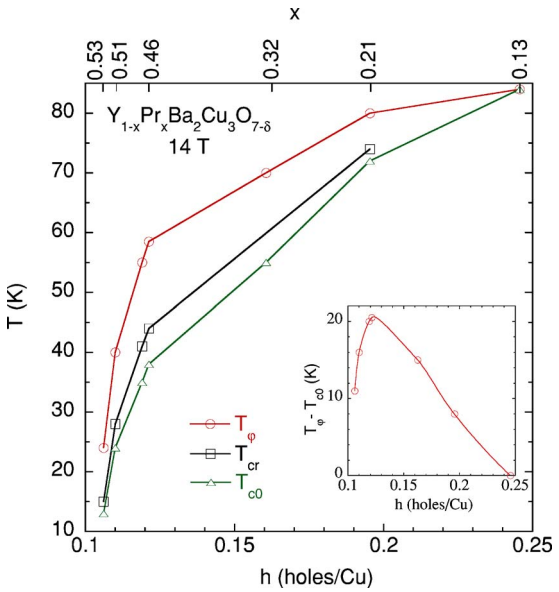

FIG. 6. (Color online) The plots of the zero-field critical temperature T_{c0}, the 2D-3D crossover temperature T_{cr}, and the temperature T_φ at which the phase correlations vanish vs hole density h of $Y_{1-x}Pr_xBa_2Cu_3O_{7-\delta}$. Inset: plot of the temperature range of phase fluctuations $\Delta T_\varphi \equiv T_\varphi - T_{c0}$. The solid lines are guides to the eye.

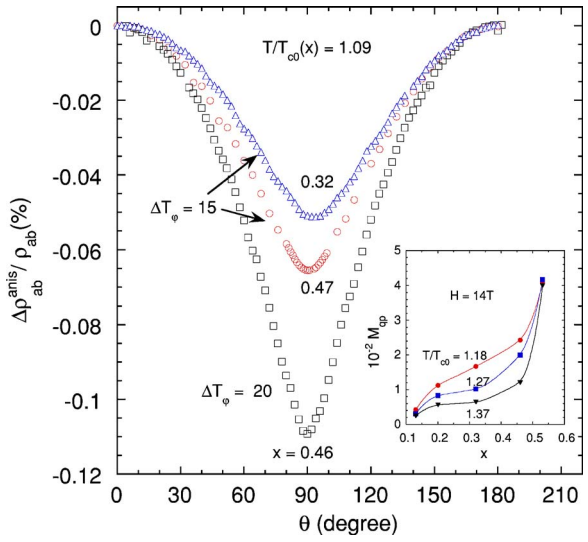

FIG. 7. (Color online) The in-plane angular magnetoresistivity $\Delta\rho^{anis}_{ab}/\rho_{ab}(0^\circ) \approx [\rho_{ab}(\theta) - \rho_{ab}(0^\circ)]/\rho_{ab}(0^\circ)$ vs angle θ between the magnetic field H and the c axis, measured at 14 T and at the same reduced temperature $T/T_{c0}(x)$ for different concentrations x of Pr. Inset: plot of coefficient M_{qp} vs doping x determined at 14 T and at the same reduced temperature $T/T_{c0}(x)$. The solid lines are guides to the eye.

on $La_{1-2x}Sr_xCuO_4$. First, while T_φ is monotonic with doping in the present data, it displays a maximum in the weakly underdoped regime in the previous measurements. Second, while T_φ and T_c merge in the slightly underdoped samples in these measurements, they merge in the slightly *overdoped* regime in the previous measurements. The reason for these differences could be the following. The present AMR signal includes both vortex and quasiparticle dissipations. With increasing T, the former contribution to dissipation decreases while the latter increases. Hence, above a certain T, the quasiparticle contribution dominates and even masks the vortex contribution. As a result these AMR measurements are less sensitive to the presence of vortices than the Nernst effect or magnetization measurements, which measure *only* the signal arising from vortex motion. On the other hand, as discussed throughout this paper, they facilitate studies that are not possible with these other two techniques.

It is interesting to note that the amplitude of the AMR curves does not follow a monotonic dependence on Pr doping. As Fig. 7 shows, the amplitude of AMR measured at a reduced temperature $T/T_{c0}(x)$ of 1.09 and a field of 14 T reaches a maximum at the same doping x at which the temperature range ΔT_φ of phase fluctuations is maximum ($x=0.46$, $h=0.12$ holes/Cu). In contrast, the quasiparticle contribution M_{qp} increases monotonically with x, with a faster increase at high Pr concentrations (see the inset to Fig. 7). Therefore, the nonmonotonic behavior of the amplitude of AMR arises only from the nonmonotonic behavior of the flux-flow term (data not shown). Furthermore, the fact that the doping dependence of ΔT_φ and M_{FF} is the same, i.e., nonmonotonic with a maximum at the same $x=0.46$ doping, indicates that the contribution of vortices (M_{FF}) to the total dissipation is enhanced for the hole density for which the temperature range of phase fluctuations ΔT_φ is maximum. This result further supports the scenario in which the flux-flow term to dissipation above T_{c0} is a result of phase fluctuations.

The increase of the quasiparticle term M_{qp} with Pr content (see the inset to Fig. 7) can be explained in the framework of the near antiferromagnetic Fermi liquid. Specifically, M_{qp} depends on the antiferromagnetic correlation length as a power law.[47] This correlation length increases with x due to the decrease of the charge carrier density with increasing Pr content. The increase becomes stronger as x increases, hence, as the antiferromagnertic transition is approached.

In summary, in-plane angular magnetoresistivity AMR measurements in magnetic fields up to 14 T on $Y_{1-x}Pr_xBa_2Cu_3O_{7-\delta}$ ($0 \leqslant x \leqslant 0.53$) single crystals facilitated the study of the nature of vortex dissipation and of the variation of its characteristics with temperature, magnetic field, and hole density. These data have shown that the vortex matter is two dimensional 2D, i.e., the resistivity depends only on the field component perpendicular to the CuO_2 planes, in the mixed state for $T < T_{c0}$, but also for $T > T_{c0}$ in the pseudogap region up to a certain temperature T_{cr}, which depends on the hole density. The fact that the 2D behavior is not lost at T_{c0} suggests not only that the c axis coherence length ξ_c does not diverge at T_{c0} but also that it is less than the interlayer spacing up to higher temperatures. For $T > T_{cr}$, there is a crossover to a three-dimensional (3D) flux line controlled dissipation. For example, this crossover occurs at $T_{cr} \approx 45$ K for the $x=0.46$ sample ($T_{c0}=38$ K, $T_\varphi=58$ K). An explicit functional dependence of magnetoresistivity, consistent with the 2D and 3D vortex matter observed in different temperature regimes, was obtained and used to study the evolution of both quasiparticle and flux-flow dissipation with T, H, and hole density. The ordinary

magnetoresistivity due to quasiparticles decreases fast with increasing T just below T_{c0} as a result of the increase of the phase space for scattering with increasing T. At $T>T_{c0}$, the quasiparticle ordinary magnetoresistivity follows a dependence which is in agreement with the near antiferromagnetic Fermi liquid model. The linear in H^2 dependence of the quasiparticle ordinary magnetoresistivity supports the validity of the expression chosen for quasiparticle conductivity, while its saturation at higher T reflects the almost cylindrical geometry of the Fermi surface. The vortexlike contribution to dissipation, M_{FF}, displays a maximum in T close to T_{c0}, which is a result of the interplay between the diffusion and inelastic relaxation rates of the order parameter. The linear dependence of M_{FF} on H at low T reflects its own definition while the nonmonotonic H dependence at high T is a result of the interplay between the number of regions able to support vorticity and the number of vortices generated by the field. The electronic phase diagram shows how high in temperature, above T_{c0}, the 2D-3D crossover and the vortexlike excitations extend for various hole densities. It also shows that both the temperature range of phase fluctuations ΔT_{φ} and the contribution M_{FF} of the vortices to the total dissipation display a maximum at a hole density of 0.12 holes/Cu ($x=0.46$). This result shows that the flux-flow resistivity (M_{FF}) is maximum in the sample with maximum phase fluctuations (ΔT_{φ}).

ACKNOWLEDGMENTS

This research was supported by the National Science Foundation under Grant No. DMR-0406471 at KSU and the U.S. Department of Energy under Grant No. DE-FG03-86ER-45230 at UCSD.

APPENDIX

Since $\rho(y)=1/\sigma(y)$ then

$$\frac{d^2\rho}{dy^2}=\frac{1}{\sigma^2}\left[\frac{2}{\sigma}\left(\frac{d\sigma}{dy}\right)^2-\frac{d^2\sigma}{dy^2}\right]. \tag{8}$$

With $\sigma(T,H,\theta)=\sigma_{qp}(T,H,\theta)+\sigma_{FF}$, Eq. (8) gives a negative convexity only if there is a real solution to the inequality:

$$\frac{d^2\sigma_{FF}}{dy^2}>\frac{2}{\sigma}\left(\frac{d\sigma_{qp}}{dy}+\frac{d\sigma_{FF}}{dy}\right)^2-\frac{d^2\sigma_{qp}}{dy^2}. \tag{9}$$

Taking $y=H|\cos\theta|$, the right hand side of the Ineq. (9) is always positive because $d^2\sigma_{qp}/dy^2<0$ [see Eq. (4)], hence $d^2\sigma_{FF}/dy^2>0$. Because $d^2\sigma_{FF}/dy^2\propto H^*(T)$, the negative curvature of $\rho(y)$ data observed [see Fig. 2 and Eq. (1)] in a certain range of temperatures $T_{c0}<T<T_{\varphi}$ is consistent with $H^*(T)\neq 0$ (note that $H^*<H_{c2}$) in this temperature range, i.e., the existence of a finite phase correlation length ξ_{φ}. Therefore, Ineq. (9) determines the temperature range over which the flux-flow contribution is nonzero. We note that Ineq. (9) has real and positive solutions as long as $(\sigma^{(2)}/\sigma)H^2\cos^2\theta \leqslant 1/12$, which is in the range of validity of Jones-Zener expansion, $\sigma^{(2)}H^2\cos^2\theta \ll \sigma_0$.

*Permanent Address: National Institute of Materials Physics, 077125 Bucharest-Magurele, Romania

[1] T. Timusk and B. Statt, Rep. Prog. Phys. **62**, 61 (1999).
[2] M. R. Norman, M. Renderia, H. Ding, and J. C. Campuzano, Phys. Rev. B **57**, R11093 (1998).
[3] Ch. Renner, B. Revaz, J. -Y. Genoud, K. Kadowaki, and Ø. Fischer, Phys. Rev. Lett. **80**, 149 (1998).
[4] J. Emery and S. A. Kivelson, Nature (London) **374** 434 (1995).
[5] C. Meingast, V. Pasler, P. Nagel, A. Rykov, S. Tajima, and P. Olsson, Phys. Rev. Lett. **89**, 229704 (2002).
[6] P. Curty and H. Beck, Phys. Rev. Lett. **91**, 257002 (2003).
[7] D. Manske, T. Dahm, and K. H. Bennemann, Phys. Rev. B **64**, 144520 (2001).
[8] T. Shibauchi, L. Krusin-Elbaum, M. Li, M. P. Maley, and P. H. Kes, Phys. Rev. Lett. **86**, 5763 (2001).
[9] J. Maly, B. Janko, and K. Levin, Phys. Rev. B **59**, 1354 (1998).
[10] H.-J. Kwon and A. T. Dorsey, Phys. Rev. B **59**, 6438 (1999).
[11] H.-J. Kwon, Phys. Rev. B **59**, 13600 (1999).
[12] M. Franz and Z. Tešanović, Phys. Rev. Lett. **87**, 257003 (2001).
[13] Z. Tešanović, O. Vafek, and M. Franz, Phys. Rev. B **65**, 180511(R) (2002).
[14] B. Bernevig, Z. Nazario, and D. I. Santiago, Philos. Mag. **84**, 2331 (2004).
[15] S. Ouazi, J. Bobroff, H. Alloul, and W. A. MacFarlane, Phys. Rev. B **70**, 104515 (2004).
[16] J. Corson, R. Malazzi, J. Orenstein, J. N. Eckstein, and I. Bozovic, Nature (London) **398**, 221 (1998).
[17] D. -N. Peligrad, M. Mehring, and A. Dulčič, Phys. Rev. B **69**, 144516 (2004).
[18] A. Lascialfari, A. Rigamonti, L. Romanó, P. Tedesco, A. Varlamov, and D. Embriaco, Phys. Rev. B **65**, 144523 (2002).
[19] Z. A. Xu, N. P. Ong, Y. Wang, T. Kakeshita, and S. Uchida, Nature (London) **406**, 486 (1998).
[20] Y. Wang, Z. A. Xu, T. Kakeshita, S. Uchida, S. Ono, Y. Ando, and N. P. Ong, Phys. Rev. B **64**, 224519 (2001).
[21] Y. Wang, N. P. Ong, Z. A. Xu, T. Kakeshita, S. Uchida, D. A. Bonn, R. Liang, and W. N. Hardy, Phys. Rev. Lett. **88**, 257003 (2002).
[22] C. Capan, K. Behnia, J. Hinderer, A. G. M. Jansen, W. Lang, C. Marcenat, C. Marin, and J. Flouquet, Phys. Rev. Lett. **88**, 056601 (2002).
[23] C. Panagopoulos, M. Majoros, and A. P. Petrović, Phys. Rev. B **69**, 144508 (2004).
[24] V. Sandu, E. Cimpoiasu, T. Katuwal, S. Li, M. B. Maple, and C. C. Almasan, Phys. Rev. Lett. **93**, 177005 (2004).
[25] T. R. Chien, T. W. Jing, N. P. Ong, and Z. Z. Wang, Phys. Rev. Lett. **66**, 3075 (1991).
[26] L. M. Paulius, B. W. Lee, M. B. Maple, and P. K. Tsai, Physica C **230**, 255 (1994).
[27] G. A. Levin, T. Stein, C. N. Jiang, C. C. Almasan, D. A. Gajewski, S. H. Han, and M. B. Maple, Physica C **282-287**, 1147 (1997).

[28] A. I. Liechtenstein and I. I. Mazin, Phys. Rev. Lett. **74**, 1000 (1995).
[29] Y. Yu, G., Cao, and Z. Jiao, Phys. Rev. B **59**, 3845 (1999).
[30] C. N. Jiang, A. R. Baldwin, G. A. Levin, T. Stein, C. C. Almasan, D. A. Gajewski, S. H. Han, and M. B. Maple, Phys. Rev. B **55**, R3390 (1997).
[31] C. C. Almasan and M. B. Maple, Phys. Rev. B **53**, 2882 (1996).
[32] Y. I. Latyshev, A. E. Koshelev, and L. N. Bulaevskii, Phys. Rev. B **68**, 134504 (2003).
[33] P. H. Kes, J. Aarts, V. M. Vinokur, and C. J. Van der Beek, Phys. Rev. Lett. **64**, 1063 (1990).
[34] H. Raffy, S. Labdi, O. Laborde, and P. Monceau, Phys. Rev. Lett. **66**, 2515 (1991).
[35] Y. Iye, A. Fukushima, T. Tamegai, T. Terashima, and Y. Bando, Physica C **185-189**, 297 (1991).
[36] X. F. Lu, Z. Wang, H. Gao, L. Shan, Y. Z. Zhang, R. T. Lu, L. Fan, S. L. Yan, Z. D. Wang, and H. H. Wen, Physica C **415**, 139 (2004).
[37] A. Barone, A. I. Larkin, and Yu. N. Ovchinnilov, J. Supercond. **3**, 155 (1990).
[38] L. Balents and D. R. Nelson, Phys. Rev. B **52**, 12951 (1995).
[39] D. S. Fisher, M. P. A. Fisher, and D. A. Huse, Phys. Rev. B **43**, 130 (1991).
[40] I. Iguchi, T. Iamaguchi, and A. Sugimoto, Nature (London) **412**, 420 (2001).
[41] S. H. Pan, J. P. O'Neal, R. L. Badzey, C. Chamon, H. Ding, J. R. Engelbrecht, Z. Wang, H. Eisaki, S. Uchida, A. K. Gupta, A. H. Ng, E. W. Hudson, K. M. Lang, and J. C. Davies, Nature (London) **413**, 282 (2001).
[42] K. M. Lang, V. Madhavan, J. E. Hoffman, E. W. Hudson, H. Eisaki, S. Uchida, and J. C. Davies, Nature (London) **415**, 412 (2002).
[43] N. E. Hussey, Eur. Phys. J. B **31**, 495 (2003).
[44] E. Cimpoiasu, G. A. Levin, C. C. Almasan, Hong Zheng, and B. W. Veal, Phys. Rev. B **63**, 104515 (2001).
[45] J. Corson, J. Orenstein, S. Oh, J. O'Donnell, and J. N. Eckstein, Phys. Rev. Lett. **85**, 2569 (2000).
[46] J. Paaske and D. V. Khveshchenko, Phys. Rev. B **57**, R8127 (1998).
[47] H. Kontani, J. Phys. Soc. Jpn. **70**, 1873 (2001).
[48] J. M. Ziman, *Electrons in Metals. A Short Guide to Fermi Surface* (Taylor & Francis Ltd., 1964) p. 69.
[49] A. I. Larkin and Yu. N. Ovchinnikov in *Nonequilibrium Superconductivity*, eds. D. N. Langenberg and A. I. Larkin (Elsevier Science Publisher, 1986). p.493
[50] J. M. Kosterlitz and D. J. Thouless, J. Phys. C **6**, 1181 (1973).
[51] P. Minnhagen, Rev. Mod. Phys. **59**, 1001 (1987).
[52] C. L. Seaman, J. J. Neumeier, M. B. Maple, L. P. Le, G. M. Luke, B. J. Sternlieb, Y. J. Uemura, J. H. Brewer, R. Kadono, R. F. Kiefl, S. R. Krietzman, and T. M. Riseman, Phys. Rev. B **42**, 6801 (1990).
[53] K. Kodama, S. Shamoto, H. Harashina, M. Sato, M. Nishi, and K. Kakurai, Physica C **263**, 333 (1996).